Targeting N-Myc in Neuroblastoma with Selective Aurora Kinase A Degraders

Jian Tang[1], Ramkumar Moorthy[1], Özlem Demir[2], Zachary D. Baker[3], Jordan A. Naumann[4], Katherine F. M. Jones[5], Michael J. Grillo[1], Ella S. Haefner[1], Ke Shi[4], Michaella J Levy[6], Hideki Aihara[4], Reuben S. Harris[4,7], Rommie E. Amaro[2], Nicholas M. Levinson[3], Daniel A. Harki[1,4,5]*

[1]Department of Medicinal Chemistry, University of Minnesota, Minneapolis, Minnesota, USA.

[2]Department of Chemistry and Biochemistry, University of California, San Diego, La Jolla, California, USA.

[3]Department of Pharmacology, University of Minnesota, Minneapolis, Minnesota, USA.

[4]Department of Biochemistry, Molecular Biology, and Biophysics, University of Minnesota, Minneapolis, Minnesota, USA.

[5]Department of Chemistry, University of Minnesota, Minneapolis, Minnesota, USA.

[6]Stowers Institute for Medical Research, Kansas City, Missouri, USA.

[7]Howard Hughes Medical Institute, University of Minnesota, Minneapolis, Minnesota, USA.

*Corresponding author, Email: daharki@umn.edu

Summary Paragraph

MYCN amplification is the most frequent genetic driver in high-risk neuroblastoma (NB) and strongly associated with poor prognosis.[1,2] The N-Myc transcription factor, which is encoded by *MYCN*, is a mechanistically validated, yet challenging target for NB therapy development.[3,4] In normal neuronal progenitors, N-Myc undergoes rapid degradation, while in *MYCN*-amplified NB cells, Aurora kinase A (Aurora-A) binds to and stabilizes N-Myc, resulting in elevated protein levels.[5,6] Allosteric Aurora-A inhibitors that displace N-Myc from binding can promote N-Myc degradation, but with limited efficacy.[7-10] Here, we report a chemical approach to decrease N-Myc levels through the targeted protein degradation of Aurora-A. A first-in-class Aurora-A/N-Myc degrader, HLB-0532259 (compound **4**), was developed from a novel Aurora-A-binding ligand that engages the Aurora-A/N-Myc complex. HLB-0532259 promotes the degradation of both Aurora-A and N-Myc with nanomolar potency and excellent selectivity and surpasses the cellular efficacy of established allosteric Aurora-A inhibitors. HLB-0532259 exhibits favorable pharmacokinetics properties and elicits tumor reduction in murine xenograft NB models. More broadly, this study delineates a novel strategy for targeting "undruggable" proteins that are reliant on accessory proteins for cellular stabilization.

The *MYCN* gene is a member of the *MYC* family and encodes the oncogenic transcription factor N-Myc. Deregulated expression of *MYCN* is associated with tumorigenesis of multiple human cancers.[2,4,11] *MYCN* amplification is the major genetic driver in high-risk neuroblastoma (NB), and represents the strongest independent adverse prognostic factor in the clinic.[1,2] Despite its critical role in NB, N-Myc remains challenging to target and represents a prototypical "undruggable" protein in drug discovery.[3,4] To date, no N-Myc-targeting therapies are available for clinical use.

In normal neuronal progenitors, N-Myc is a short-lived protein with a half-life of 30-50 mins.[5] During the cell cycle, after sequential phosphorylation at S62 and T58 followed by dephosphorylation of S62, N-Myc is tightly controlled for proteasomal degradation in M-phase by the E3 ubiquitin ligase SCF^{Fbxw7}.[12] However, N-Myc has a significantly prolonged half-life in *MYCN*-amplified NB cells that results in elevated steady-state protein levels.[6] The mechanism of stabilization is conferred by Aurora kinase A (Aurora-A) binding to the N-Myc/SCF^{Fbxw7} complex and interfering with SCF^{Fbxw7}-mediated ubiquitination on N-Myc. Moreover, N-Myc binds specifically to the active conformation of Aurora-A.[6,13] Several allosteric Aurora-A inhibitors, such as MLN8237 (alisertib) and CD532, have been found to promote N-Myc degradation by distorting the active conformation of the kinase to disrupt the Aurora-A/N-Myc complex.[7,8] However, these compounds function with a negative cooperativity against N-Myc, which may explain their limited efficacy when N-Myc is highly expressed.[10,13] Results from recent phase II clinical trials showed an inferior response of MLN8237 in patients with *MYCN*-amplification status.[9] Therefore, developing Aurora-A modulators with greater effects on N-Myc protein stability is urgently needed.

Short hairpin RNA knockdown of Aurora-A significantly down-regulates N-Myc levels in *MYCN*-amplified NB.[6] Therefore, we explored the targeted protein degradation of Aurora-A as a novel chemical approach to destabilize N-Myc. We hypothesize that with Aurora-A being degraded, unbound N-Myc, even at high expression levels, will be rapidly eliminated through its native degradation pathway (Fig. 1a). We applied proteolysis-targeting chimera (PROTAC) technology to develop Aurora-A/N-Myc degraders. PROTACs are heterobifunctional molecules comprised of a recognition moiety for a protein of interest (POI) and an E3 ubiquitin ligase ligand connected via a chemical linker. By co-opting the ubiquitin-proteasome system (UPS), these molecules function through proximity induced polyubiquitination of the POI and subsequent proteasome-dependent degradation (Fig. 1a).[14,15]

Development of Aurora-A/N-Myc degraders

We reasoned that current Aurora-A inhibitors were not optimal to develop selective Aurora-A/N-Myc degraders. First, most type I/DFG-in Aurora-A inhibitors binding to its active state suffer from poor selectivity against the homolog Aurora-B and/or other structurally related kinases.[16] Second, type II/DFG-out Aurora-A inhibitors are

highly selective, but they are incompatible with the active conformation of Aurora-A when bound to N-Myc (*i.e.* negative cooperativity), suggesting PROTACs derived from these inhibitors would have limited efficacy at degrading the Aurora-A/N-Myc pool.[13] Indeed, several MLN8237-based Aurora-A PROTACs have been reported recently, but no evidence demonstrates their capability in promoting N-Myc degradation.[17-19]

To address this issue, a novel Aurora-A ligand was developed from the FDA-approved drug ribociclib (Fig. 1b, **1**), a highly selective inhibitor targeting Cyclin-dependent kinase 4/6 (CDK4/6).[20] Chemical modifications of the pyridinylpiperazine moiety of ribociclib resulted in the discovery of ligand **2**, which showed an approximate 1000-fold increase of binding affinity against Aurora-A with a dissociation constant (K_d) value of 0.85 nM. Next, PROTAC **4** was developed by conjugating **2** through a hexyloxy linker with the widely used thalidomide, which targets cereblon (CRBN), the substrate receptor of the $CRL4^{CRBN}$ E3 ubiquitin ligase.[21] **4** maintained a strong affinity for Aurora-A (K_d = 6.3 nM) and exhibited an 8-fold selectivity against CDK4-CyclinD1 (Fig. 1b-c). N-Methylation on the glutarimide group of thalidomide has been shown to abolish its binding to CRBN,[22] and such modification yielded the inactive PROTAC **5** that shares similar binding and inhibitory profiles as **4** against Aurora-A and CDK4 (Fig. 1b-c and Extended Data Fig. 1a). The presence of the pyridine nitrogen in ribociclib (highlighted in red, Fig. 1b) is critical for its high CDK4/6 selectivity over other kinases.[23] Installation of this nitrogen atom as shown in **3** is more detrimental to Aurora-A binding (~400-fold decrease) than CDK4-CyclinD1 (14-fold decrease, Fig. 1b-c and Extended Data Fig. 1a). A similar design strategy was applied to **3** to develop another inactive PROTAC **6** (Fig. 1b). **5** and **6** were used in the following studies as controls as they show no or weak binding to CRBN and Aurora-A, respectively.

When screened against a panel of 468 kinases at 1 μM concentration, ~160-fold above its K_d value against Aurora-A, **4** displayed an excellent target selectivity with S(10) and S(1) scores of 0.015 and 0.002, respectively (Fig. 1d, and Extended data Fig. 1b). In particular, **4** has a 25-fold selectivity against Aurora-B (K_d = 160 nM). Other potential off-target kinases (K_d < 200 nM) include Aurora-C, CDK4, CDK9, EPHB6, and TrkA (Extended data Fig. 1c).

4 is a potent Aurora-A degrader

MYCN-non-amplified cancer cell lines were used initially to characterize **4** for degrading Aurora-A in the absence of N-Myc. A rapid degradation of Aurora-A with a short half-life ($t_{1/2}$) of 2 h was observed in MCF-7 breast cancer cells after the treatment of **4** at 0.1 μM (Extended data Fig. 1d-e). After a 4 h treatment, the concentration of **4** needed to degrade half of the protein (DC_{50}) for Aurora-A is 20.2 nM with a maximum level of degradation (D_{max}) of 94%, while less effective CDK4 degradation was observed (Fig. 1e, and Extended data Fig. 1f-h). Of note, **4** displayed a lower activity in degrading Aurora-A at a high concentration (*e.g.* 2 μM), reflecting the characteristic "hook-effect" of a bifunctional degrader.[14,15] Interestingly, the potency of **4** for Aurora-A

degradation showed only slight differences across cell lines with various CRBN levels, suggesting that effective degradation of Aurora-A can be achieved by PROTACs at a low fractional engagement of the E3 ligase due to their catalytic nature (Extended data Fig. 1i-j).[14] Subsequent mechanistic studies validated that Aurora-A degradation by **4** requires concurrent target engagement of both Aurora-A and CRBN, and is indeed dependent on the activity of the UPS (Fig. 1f).

2 & 4 binds to the AURKA/N-Myc complex

After validating **4** as a *bona fide* Aurora-A degrader, we next assessed whether **2** and **4** show target engagement of the Aurora-A/N-Myc complex. Therefore, crystallography studies were first performed to probe the binding of the newly discovered Aurora-A ligands. **2** was successfully co-crystallized with the Aurora-A kinase domain at 1.8 Å resolution and found to occupy the ATP-binding site (Fig. 2a). The 4-aminopyrimidine moiety of **2** forms two key H-bond interactions with the backbone of A213 on the hinge region of Aurora-A, and the oxygen atom of the *N*,*N*-dimethylamide group forms another critical H-bond with the catalytic K162 residue. In addition, the *N*-methyl amide on the benzene ring sits at the solvent-exposed site and forms H-bond networks with nearby hydrophilic residues via water molecules (Fig. 2b). A similar binding mode was observed with ligand **3**.

Aurora-A adopts an active DFG-in and αC-helix-in conformation when bound to N-Myc or the co-activator TPX2, while allosteric inhibitors, such as MLN8504 (a MLN8237 analogue) or CD532, induce a displacement of the αC-helix and disrupt the binding of N-Myc with Aurora-A. Interestingly, **2** stabilizes an inactive DFG-out conformation of Aurora-A (Fig. 2a), but unlike the crystal structures with MLN8504 or CD532, Aurora-A maintains a closed conformation (αC-helix-in) when bound to **2**, similar to the conformation with N-Myc or VX-680, a DFG-in inhibitor in the presence of TPX2 (Fig. 2c). In addition, allosteric inhibitors induce significant shifts of residues that directly interact with N-Myc, including K143, Y334, Q335 and Y338,[13] and such conformational changes were not observed in the Aurora-A:**2** co-crystal structure (Extended data Fig. 2c). Our previous studies have shown the structural plasticity of Aurora-A and its conformation may differ from the crystallized form when coupled with another binding partner (*e.g.,* TPX2).[24] Taken together, these findings suggest that **2** is a weak DFG-out binder and may not disrupt the structural features on Aurora-A required for N-Myc binding.

To test this hypothesis, we first performed a previously reported *in vitro* pull-down assay with recombinant Aurora-A protein and a biotinylated N-Myc peptide (residues 61-89).[13] We found that ligand **2** showed significantly less competition against the N-Myc peptide than MLN8237 for binding Aurora-A (Extended data Fig. 3a-b). Next, a biolayer interferometry (BLI) ternary binding assay was used to quantify the interaction between **4** and the Aurora-A/N-Myc complex. Biotinylated N-Myc peptide was loaded onto streptavidin-coated biosensors and dipped into a solution containing recombinant Aurora-A. After washing off excess protein, the

preformed complex was dipped into a solution containing **4** to measure the association, then in buffer to measure the dissociation (Extended data Fig. 3c-d). Calculated affinity (K_d) of **4** for the Aurora-A/N-Myc complex was 19.5 nM, which is in agreement with the binding affinity previously determined for the binary interaction between **4** and Aurora-A (Fig. 2d-e). In contrast, titration of MLN8237 results in a concentration-dependent decrease in signal, demonstrating its ability to disrupt the Aurora-A/N-Myc interaction (Extended Fig. 3e). Furthermore, pull-down experiments with **2**-PEG3-Biotin and lysates from *MYCN*-amplified neuroblastoma SK-N-BE(2) cells showed the enrichment of both endogenous Aurora-A and N-Myc, indicating the target engagement of **2**-PEG3-Biotin to the Aurora-A/N-Myc complex (Fig. 2f). Following computational studies generated a model of the N-Myc/Aurora-A/**4**/CRBN quaternary complex, which corroborated N-Myc binding does not compete with **4** binding to Aurora-A (Extended Fig. 3f). Taken together, these data suggest the uncompetitive binding mode of **4** with Aurora-A/N-Myc complex.

4 degrades N-Myc in *MYCN*-amplified NB

In *MYCN*-amplified NB SK-N-BE(2) cells, **4** induces rapid and potent degradation of Aurora-A with a concomitant N-Myc degradation (Fig. 3a, and Extended Data Fig. 4a-c). After 4 hours, the apparent DC_{50} values ($DC_{50,\ app}$) for N-Myc were 179 nM and 229 nM in SK-N-BE(2) and Kelly cells, respectively (Fig. 3b-c, and Extended Data Fig. 4d). In contrast, inactive PROTAC **5** did not affect the protein levels of either Aurora-A or N-Myc (Extended Data Fig. 4e). Interestingly, N-Myc degradation did not occur until a substantial amount of Aurora-A ($\geq$ 75%) had been degraded, suggesting near complete Aurora-A degradation (*i.e.* a high D_{max} value) is required to degrade N-Myc. This was further validated by a washout experiment, in which both Aurora-A and N-Myc were depleted first by **4**. After replacing **4** with fresh media, even a small portion of recovered Aurora-A could fully stabilize N-Myc to its steady-state level (Extended Data Fig. 4f). All previously reported Aurora-A PROTACs use MLN8237 as the Aurora-A binding portion, suggesting their limited access to Aurora-A pools that are coupled with other binding partners, such as TPX2 and N-Myc. This could potentially explain their relatively low D_{max} values for Aurora-A and ineffectiveness in promoting N-Myc degradation (*e.g.,* JB170, Extended Data Fig. 4g).[17-19]

We further demonstrated that N-Myc degradation by **4** also requires target engagement of both Aurora-A and CRBN and depends on the activity of the UPS (Extended Data Fig. 5a). In *MYCN*-amplified NB cells, poly-ubiquitinated N-Myc is rescued by the ubiquitin-specific protease 7 (USP7) through deubiquitylation,[25] and co-treatment with a selective USP7 inhibitor, FT671,[26] indeed showed synergistic effects with **4** for degrading N-Myc (Extended Data Fig. 5b-c). Furthermore, in *MYCN*-non-amplified NB cells, **4** did not degrade the homolog c-Myc despite potent Aurora-A degradation, suggesting its activity for degrading N-Myc depends on the regulatory mechanism of Aurora-A (Extended Data Fig. 5d). Taken together, these findings validate the

hypothesized mode-of-action model of **4**, in which N-Myc is degraded via its native degradation pathway after Aurora-A depletion (Fig. 1a).

With its novel mechanism, **4** outperformed MLN8237 and CD532 to induce more potent N-Myc degradation in a head-to-head comparison experiment (Fig. 3d, and Extended Data Fig. 5e). An established hallmark for selective Aurora-A inhibition over Aurora-B is an initial increase of phosphorylated histone H3 (p-H3) at lower concentrations of inhibitors, followed by a drastic reduction at higher concentrations.[8,27] **4** significantly upregulated p-H3 levels spanning a broad range of concentrations, indicating its high *in cellulo* selectivity for Aurora-A over Aurora-B (Fig. 3d, and Extended Data Fig. 5e). Additionally, consistent with previous studies, MLN8237 treatment leads to abnormal high expression of Aurora-A, which in turn could potentially lower its expected efficacy to destabilize N-Myc.[28] In contrast, treatment with degrader **4** maintained low levels of Aurora-A despite upregulated transcription similarly as MLN8237 (Fig. 3d-e, and Extended Data Fig. 5e-f). These data suggest the additional advantage of Aurora-A degradation over inhibition for destabilizing N-Myc. Of note, **4** did not affect *MYCN* mRNA levels, suggesting the decreased N-Myc protein levels is not due to its transcriptional inhibition (Fig. 3e, and Extended Data Fig. 5f).

To assess the proteome-wide degradation selectivity of **4**, we performed a quantitative multiplexed proteomic analysis using Tandem Mass Tag (TMT) isobaric labeling tags. More than 6000 protein IDs were quantified in this study, and Aurora-A and N-Myc were found among the most significantly downregulated group (Fig. 3f). Most other proteins that were downregulated $\geq$ 35% belong to either N-Myc or Aurora-A associated genes, such as the 60S ribosomal subunits (Extended Data Fig. 5g).[29,30] Despite its *in vitro* binding to several other kinases to various degrees (Extended data Fig. 1c), **4** did not result in significant decrease of their protein levels (Fig. 3f, green spots). The high selectivity over these kinases was also confirmed by immunoblotting in both NB and non-NB cells (Fig. 3g, and Extended Data 5h).

4 for treating *MYCN*-amplified NB

Aurora-A is a key regulator of p53 homeostasis in TP53 wild-type ($TP53^{wt}$) cells through its kinase activity, while stabilizing N-Myc in a kinase-independent manner (*i.e.,* scaffolding function).[6,31] Treatment with **4** in $TP53^{wt}$ IMR-32 cells significantly stabilized p53, along with decreased Aurora-A and N-Myc. Similar effects were observed for their respective downstream signaling components, such as increased $p21^{Cip1}$ and decreased Cyclin D levels (Fig. 4a-b). The effects of **4** on the p53 pathway was also confirmed in another $TP53^{wt}$ cell line, MCF-7 (Extended Data Fig. 6a). Control **5**, which only inhibits Aurora-A kinase activity but not its scaffolding function, increased p53 and p21 (albeit with a lower potency than **4**) but did not affect N-Myc and Cyclin Ds (Extended Data Fig. 6b). Moreover, in IMR-32 cells, **4** upregulated the transcriptional levels of *CDKN1A* (encoding $p21^{Cip1}$)

and *PLK2*, two p53 target genes, and downregulated *MAD2L1*, a direct target gene of N-Myc (Extended Data Fig. 6c). In line with these studies, in TP53 mutant cell lines SK-N-BE(2) and Kelly**, 4** only decreased the levels of N-Myc and Cyclin Ds but did not affect p53 levels despite Aurora-A degradation (Extended Data Fig. 6d-e). Collectively, these data indicated the on-target effects of **4** modulating p53 and N-Myc pathways through Aurora-A degradation.

MYCN-amplified NB cells underwent apoptosis after the treatment of **4**, indicated by the cleavage of PARP-1 and Caspase-3 (Fig. 4c). **4** also exhibited potent cytotoxicity against a panel of *MYCN*-amplified NB cells with IC_{50} values ranging from 20.1 nM to 131 nM (Fig. 4d and Extended Data Fig. 6f). However, **4** was much less effective in the *MYCN*-non-amplified NB cell line SK-N-AS, which is known to be resistant against Aurora-A knockdown (Extended Data Fig. 6f).[6] Notably, the inactive PROTAC **5** is less potent at inducing apoptosis and exhibits much lower cytotoxicity than **4** (Fig. 4c-d, Extended Data Fig. 6f).

Pharmacokinetic studies in CD-1 male mice showed that **4** has a long half-life and a high total drug exposure after 10 mg/kg dosing via intraperitoneal (IP) injection (Fig. 4e). We next evaluated the *in vivo* anti-tumor efficacy of **4** in a xenograft mice model of *MYCN*-amplified neuroblastoma. We found that IP treatment of **4** every 2 days or every 3 days significantly delayed the growth of SK-N-BE(2) tumors engrafted into the subcutaneous flanks of nude mice (Fig. 4f). Nine days after the onset of treatment, the mice injected every 3 days showed substantial tumor regression (mean = 50.8 mm^3), and the mice injected every 2 days demonstrated a moderate reduction in tumor volume (mean = 124.9 mm^3), compared to the vehicle treated mice (mean = 374.4 mm^3, Fig. 4g).

Conclusion

MYCN amplification in neuroblastoma patients is strongly associated with disease aggressiveness and low survival rates.[1,2] Aurora-A stabilizes N-Myc in *MYCN*-amplified NB cells and genetic knockdown of Aurora-A decreases N-Myc protein levels.[6] Based on this genetic validation, we report a chemical strategy to degrade N-Myc through the targeted protein degradation of Aurora-A. We first developed a novel Aurora-A-targeting ligand **2** with high affinity and specificity. Elaboration of **2** to heterobifunctional degrader **4** resulted in a compound with strong Aurora-A engagement that is not competitive with N-Myc binding. Furthermore, **4** is highly effective in degrading N-Myc and distinguished from other reported Aurora-A degraders developed from the competitive modulator MLN8237,[17-19] which possess comparatively low maximum degradation levels (D_{max}) of Aurora-A that failed to result in the concomitant degradation of N-Myc. Our data support our working hypothesis that Aurora-A-binding ligands that are not competitive with N-Myc binding are required. The first-in-class Aurora-A/N-Myc degrader **4** induces a rapid and potent degradation of both Aurora-A and N-Myc in neuroblastoma cells. Additional studies demonstrate that **4** exhibits a high degradation selectivity, on-target modulating effects, and therapeutic potential against *in vitro* and *in vivo* neuroblastoma models. Taken together, this study provides a

novel lead compound for neuroblastoma therapy development and demonstrates that "undruggable" proteins, such as N-Myc, may be modulated through the degradation of their regulatory binding partners.

Acknowledgements:

We gratefully acknowledge funding from the Department of Defense (W81XWH-21-1-0674 to D.A.H., R.S.H, R.E.A. and N.M.L. and W81XWH-19-1-0336 to J.T.), the American Association for Cancer Research – Bayer Innovation and Discovery Grant Program (21-80-44-HARK to D.A.H.), the National Institute of Health (P01-CA234228 to D.A.H., H.A., R.S.H., and R.E.A.), and the University of Minnesota, Office of Discovery and Translation (award to D.A.H.), which is supported by the National Institutes of Health, National Center for Advancing Translational Sciences (UL1TR002494). J.T. thanks the University of Minnesota for a Doctoral Dissertation Fellowship and the University of Minnesota, College of Pharmacy, for a Bighley Graduate Fellowship. K.F.M.J. acknowledges the National Science Foundation, Graduate Research Fellowship Program.

Author Contributions:

D.A.H. and J.T. conceived the study and designed the overall strategy with guidance from N.M.L.; J.T. and R.M. designed and synthesized the compounds; J.T. and E.S.H. conducted cell-based experiments; Ö.D. performed the computational modeling studies with guidance by R.E.A.; Z.D.B. expressed recombinant proteins and performed crystallography with K.S., which was also guided by N.M.L. and H.A.; J.A.N. performed the animal studies with guidance by R.S.H.; K.F.M.J. performed the proteomics study and analyzed proteomic data with M.J.L.; and M.J.G. designed and ran the BLI assay. J.T. and D.A.H. wrote the manuscript with input from all authors.

Competing interests

Compounds **2**-**6** and associated data are covered in a patent filed by the University of Minnesota, *"Compounds that degrade kinases and uses thereof"*, PCT/US2020/035977. D.A.H., J.T., R.M., Ö.D., and R.E.A. are inventors. The authors declare no other competing financial interests.

References

1 Brodeur, G. M., Seeger, R. C., Schwab, M., Varmus, H. E. & Bishop, J. M. Amplification of N-myc in Untreated Human Neuroblastomas Correlates with Advanced Disease Stage. *Science* **224**, 1121-1124 (1984).

2 Huang, M. & Weiss, W. A. Neuroblastoma and MYCN. *Cold Spring Harb Perspect Med* **3**, a014415, doi:10.1101/cshperspect.a014415 (2013).

3 Wolpaw, A. J. *et al.* Drugging the "Undruggable" MYCN Oncogenic Transcription Factor: Overcoming Previous Obstacles to Impact Childhood Cancers. *Cancer Res* **81**, 1627-1632, doi:10.1158/0008-5472.CAN-20-3108 (2021).

4 Rickman, D. S., Schulte, J. H. & Eilers, M. The Expanding World of N-MYC-Driven Tumors. *Cancer Discov* **8**, 150-163, doi:10.1158/2159-8290.CD-17-0273 (2018).

5 Bonvini, P., Nguyen, P., Trepel, J. & Neckers, L. M. In vivo degradation of N-myc in neuroblastoma cells is mediated by the 26S proteasome. *Oncogene* **16**, 1131-1139 (1998).

6 Otto, T. *et al.* Stabilization of N-Myc is a critical function of Aurora A in human neuroblastoma. *Cancer Cell* **15**, 67-78, doi:10.1016/j.ccr.2008.12.005 (2009).

7 Brockmann, M. *et al.* Small molecule inhibitors of aurora-a induce proteasomal degradation of N-myc in childhood neuroblastoma. *Cancer Cell* **24**, 75-89, doi:10.1016/j.ccr.2013.05.005 (2013).

8 Gustafson, W. C. *et al.* Drugging MYCN through an allosteric transition in Aurora kinase A. *Cancer Cell* **26**, 414-427, doi:10.1016/j.ccr.2014.07.015 (2014).

9 Beltran, H. *et al.* A Phase II Trial of the Aurora Kinase A Inhibitor Alisertib for Patients with Castration-resistant and Neuroendocrine Prostate Cancer: Efficacy and Biomarkers. *Clin Cancer Res* **25**, 43-51, doi:10.1158/1078-0432.CCR-18-1912 (2019).

10 Naso, F. D. *et al.* Nuclear localisation of Aurora-A: its regulation and significance for Aurora-A functions in cancer. *Oncogene* **40**, 3917-3928, doi:10.1038/s41388-021-01766-w (2021).

11 Liu, R., Shi, P., Wang, Z., Yuan, C. & Cui, H. Molecular Mechanisms of MYCN Dysregulation in Cancers. *Front Oncol* **10**, 625332, doi:10.3389/fonc.2020.625332 (2020).

12 Adhikary, S. & Eilers, M. Transcriptional regulation and transformation by Myc proteins. *Nat Rev Mol Cell Biol* **6**, 635-645, doi:10.1038/nrm1703 (2005).

13 Richards, M. W. *et al.* Structural basis of N-Myc binding by Aurora-A and its destabilization by kinase inhibitors. *Proc Natl Acad Sci U S A* **113**, 13726-13731, doi:10.1073/pnas.1610626113 (2016).

14 Bondeson, D. P. *et al.* Catalytic in vivo protein knockdown by small-molecule PROTACs. *Nat Chem Biol* **11**, 611-617, doi:10.1038/nchembio.1858 (2015).

15 Burslem, G. M. & Crews, C. M. Proteolysis-Targeting Chimeras as Therapeutics and Tools for Biological Discovery. *Cell* **181**, 102-114, doi:10.1016/j.cell.2019.11.031 (2020).

16 Du, R., Huang, C., Liu, K., Li, X. & Dong, Z. Targeting AURKA in Cancer: molecular mechanisms and opportunities for Cancer therapy. *Mol Cancer* **20**, 15, doi:10.1186/s12943-020-01305-3 (2021).

17 Adhikari, B. *et al.* PROTAC-mediated degradation reveals a non-catalytic function of AURORA-A kinase. *Nat Chem Biol* **16**, 1179-1188, doi:10.1038/s41589-020-00652-y (2020).

18 Wang, R. *et al.* Selective targeting of non-centrosomal AURKA functions through use of a targeted protein degradation tool. *Commun Biol* **4**, 640, doi:10.1038/s42003-021-02158-2 (2021).

19 Donovan, K. A. *et al.* Mapping the Degradable Kinome Provides a Resource for Expedited Degrader Development. *Cell* **183**, 1714-1731 e1710, doi:10.1016/j.cell.2020.10.038 (2020).

20 Chen, P. *et al.* Spectrum and Degree of CDK Drug Interactions Predicts Clinical Performance. *Mol Cancer Ther* **15**, 2273-2281, doi:10.1158/1535-7163.MCT-16-0300 (2016).

21 Fischer, E. S. *et al.* Structure of the DDB1-CRBN E3 ubiquitin ligase in complex with thalidomide. *Nature* **512**, 49. PMID 25043012, doi:10.1038/nature13527 (2014).

22 Lu, J. *et al.* Hijacking the E3 Ubiquitin Ligase Cereblon to Efficiently Target BRD4. *Chem Biol* **22**, 755. PMID 26051217, doi:10.1016/j.chembiol.2015.05.009 (2015).

23 Ammazzalorso, A., Agamennone, M., De Filippis, B. & Fantacuzzi, M. Development of CDK4/6 Inhibitors: A Five Years Update. *Molecules* **26**, doi:10.3390/molecules26051488 (2021).

24 Lake, E. W. *et al.* Quantitative conformational profiling of kinase inhibitors reveals origins of selectivity for Aurora kinase activation states. *Proc Natl Acad Sci USA* **115**, E11894-E11903, doi:10.1073/pnas.1811158115 (2018).

25 Tavana, O. *et al.* HAUSP deubiquitinates and stabilizes N-Myc in neuroblastoma. *Nat Med* **22**, 1180-1186, doi:10.1038/nm.4180 (2016).

26 Turnbull, A. P. *et al.* Molecular basis of USP7 inhibition by selective small-molecule inhibitors. *Nature* **550**, 481-486, doi:10.1038/nature24451 (2017).

27 Wen, Q. *et al.* Identification of regulators of polyploidization presents therapeutic targets for treatment of AMKL. *Cell* **150**, 575-589, doi:10.1016/j.cell.2012.06.032 (2012).

28 Yang, Y. *et al.* Silencing of AURKA augments the antitumor efficacy of the AURKA inhibitor MLN8237 on neuroblastoma cells. *Cancer Cell Int* **20**, 9, doi:10.1186/s12935-019-1072-y (2020).

29 Boon, k. *et al.* N-myc enhances the expression of a large set of genes functioning in ribosome biogenesis and protein synthesis. *The EMBO Journal* **20**, 1383-1393 (2001).

30 van Riggelen, J., Yetil, A. & Felsher, D. W. MYC as a regulator of ribosome biogenesis and protein synthesis. *Nat Rev Cancer* **10**, 301-309, doi:10.1038/nrc2819 (2010).

31 Katayama, H. *et al.* Phosphorylation by aurora kinase A induces Mdm2-mediated destabilization and inhibition of p53. *Nat Genet* **36**, 55-62, doi:10.1038/ng1279 (2004).

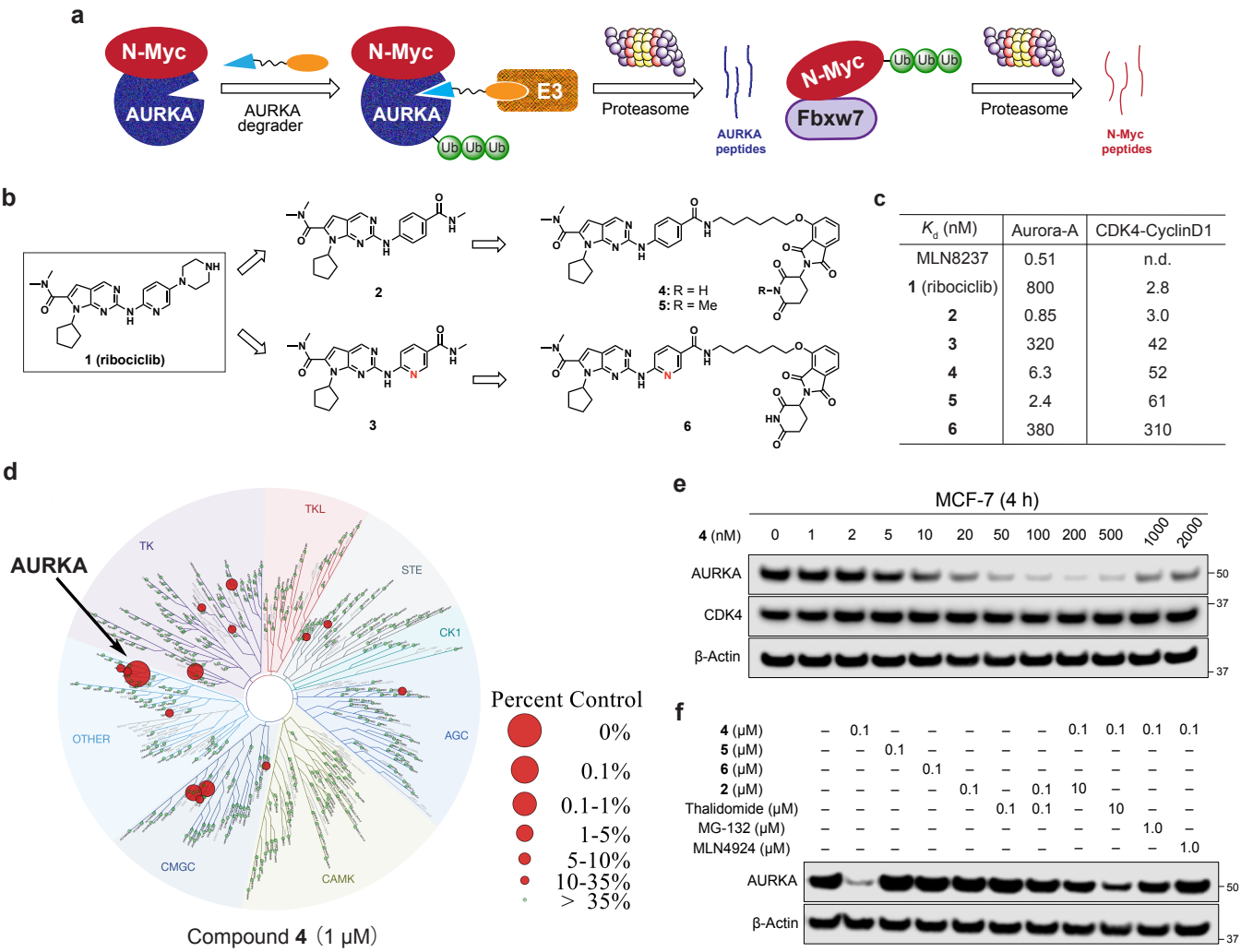

K_d (nM)	Aurora-A	CDK4-CyclinD1
MLN8237	0.51	n.d.
1 (ribociclib)	800	2.8
2	0.85	3.0
3	320	42
4	6.3	52
5	2.4	61
6	380	310

Figure 1 | Discovery of novel Aurora-A degraders. **A**, Conceptual model of N-Myc depletion through targeted protein degradation of Aurora-A (AURKA). Fbxw7: the substrate receptor of the SCF^{Fbxw7} E3 ubiquitin ligase. **b**, Discovery of novel Aurora-A ligands **2** and **3**, and Aurora-A PROTACs **4**, **5**, and **6** through chemical modifications of the CDK4/6 inhibitor **1** (ribociclib). **c**, Binding affinity (K_d) for Aurora-A and CDK4-Cyclin D1. Data are the average of two independent biological replicates. **d**, The KINOMEscan TREEspot map demonstrating the selectivity profiles of **4** against a panel of 468 kinases. See Extended Data Fig. 1a for a full spectrum including atypical, mutant, lipid, and pathogen kinases. **e**, **4** induces the degradation of Aurora-A but not CDK4 in MCF-7 cells. Representative figure, n = 4. See Extended Data Fig. 1f for the degradation curves. **f**, Mechanistic studies of Aurora-A degradation by **4** in MCF-7 cells after 4 h. Representative figure, n = 3. Thalidomide: a CRBN ligand; MG-132: a proteasome inhibitor; MLN4924: a neddylation inhibitor that blocks the function of Cullin ring E3 ligases. For the competition set-up (the four lanes on the right side), cells were pre-treated with **2**, thalidomide, MG-132 or MLN4924 for 1 h, respectively, before adding **4** (0.1 μM) for additional 4 h.

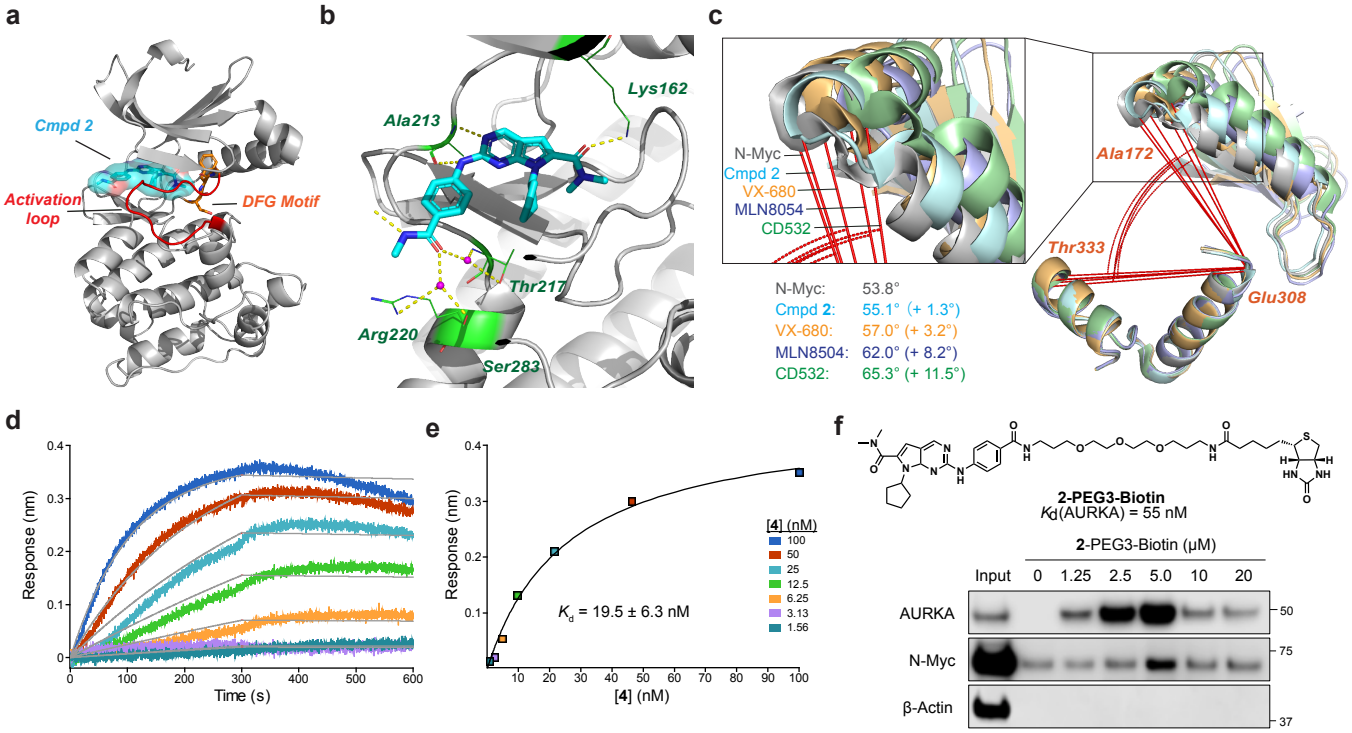

Figure 2 | 2 and 4 bind to Aurora-A/N-Myc complex. **a-b**, The co-crystal structure of **2** with Aurora-A 122-403 (PDB: To Be Provided). Ligand **2** is shown in cyan, activation loop in red, DFG motif in orange, and residues that form H-bond with **2** in green. **c**, Angle between α-Cs of T33, E308 and A172 of Aurora-A[8] when co-crystallized with N-Myc peptide (PDB: 5G1X, grey), **2** (PDB: XXX, cyan), VX-680 (PDB: 3E5A, orange), MLN8504 (PDB: 2WTV, blue) and CD532 (PDB: 4J8M, green). Values in the parenthesis indicate the angle difference from the Aurora-A/N-Myc conformation. **d-e**, BLI ternary binding assay with **4** binding to the biotinylated N-Myc peptide/Aurora-A complex. n = 2. **f**, Chemical structure of **2**-PEG3-Biotin and representative figure of the enrichment of endogenous Aurora-A and N-Myc in SK-N-BE(2) cell lysates with **2**-PEG3-Biotin. n = 3.

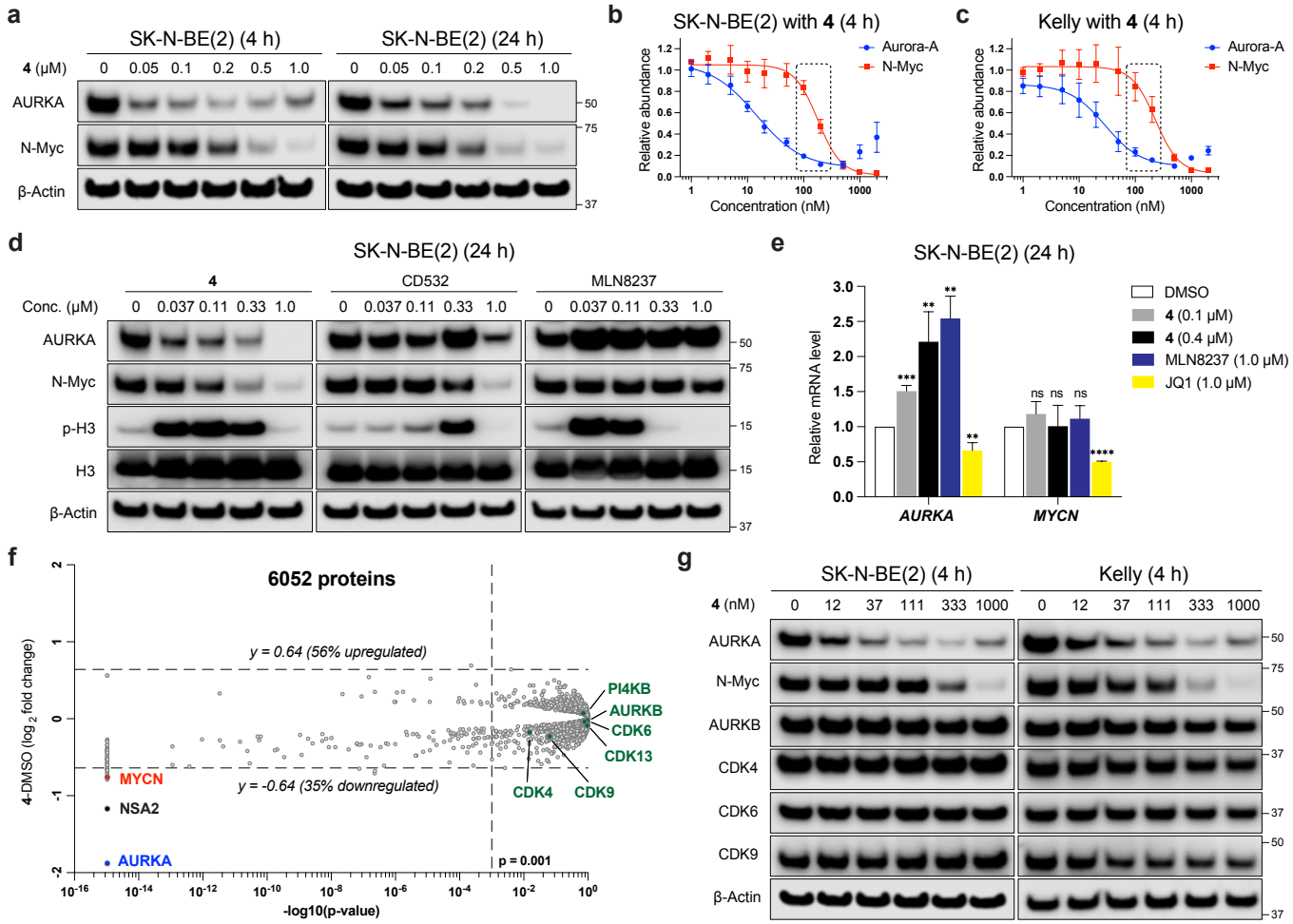

Figure 3 | 4 induces N-Myc degradation in *MYCN*-amplified NB cells. a, Concomitant degradation of Aurora-A and N-Myc by **4** in SK-N-BE(2) cells after 4 h and 24 h. n = 3. **b-c**, Degradation curves of **4** for Aurora-A and N-Myc in SK-N-BE(2) and Kelly cell lines after 4 h. Dashed boxes indicate the concentration range where N-Myc degradation starts. See Extended Data Figure 3 for DC_{50} and D_{max} values. n = 3. Degradation curves represent mean ± s.e.m. **d**, Head-to-head comparison of **4** with MLN8237 and CD532 for their effects on the protein level changes of Aurora-A, N-Myc, p-H3 in SK-N-BE(2) cells after 24 h. n = 3. **e**, Relative mRNA levels of *AURKA* and *MYCN* in SK-N-BE(2) cells after the treatment with **4**, MLN8237, or a BET inhibitor JQ1 for 24 h by RT-qPCR. n = 3. Bars represent mean ± s.d. **p < 0.01, ***p < 0.001, ****P < 0.0001. **f**, Scatter plot showing changes in protein abundance in SK-N-BE(2) cells with **4** (0.4 μM) versus DMSO control after 4 h treatment by TMT-based quantitative proteomic profiling. Significant changes were assessed by background-based t-test in Proteome Discoverer with the $\log_2$ fold change on the y-axis, and negative $\log_{10}$ p values on the x-axis from two independent biological replicates. See Supplementary Table 3 for a full list of identified proteins. **g**. Immunoblotting of Aurora-A, N-Myc, and other kinases in SK-N-BE(2) and Kelly cells after the treatment with **4** for 4 h. n = 3.

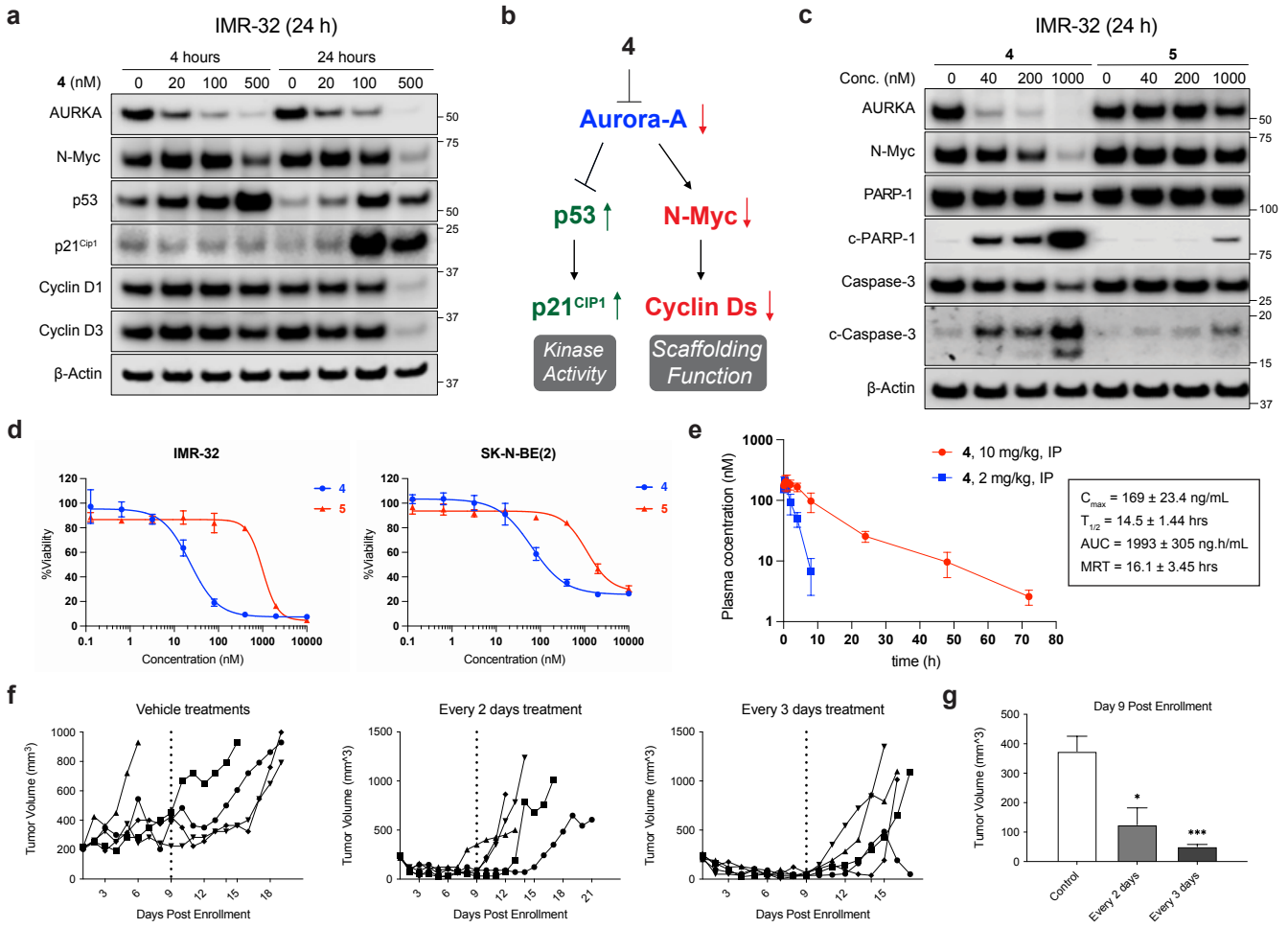

Figure 4 | *In vitro* and *in vivo* therapeutic effects of 4 for NB. a-b, **4** upregulates tumor suppressor proteins p53 and $p21^{Cip1}$, and downregulates oncoproteins N-Myc and CyclinDs in $TP53^{wt}$ IMR-32 cells after 24 h. n = 3. **c**, Immunoblotting of the cleaved PARP-1 and cleaved Caspase-3 as apoptotic markers after the treatment with **4** and **5** for 24 h in IMR-32 cells. n = 3. **d**, Cytotoxicity of **4** and **5** in SK-N-BE(2) and IMR-32 cells by Alamar Blue assay. n =3. **e**, Pharmacokinetic profiling of **4** in CD-1 male mice via intraperitoneal injection. Data represent mean ± s.d. from four mice in each dosing group. **f-g**, SK-N-BE(2) tumor growth in female nude mice treated with **4** via intraperitoneal injection every 2 or 3 days, or vehicle every 2 days. Bars represent mean ± s.d. *p < 0.05, ***p < 0.001.

a

IC_{50} (nM)	Aurora-A	CDK4-CyclinD1
MLN8237	< 0.051	n.d.
1 (ribociclib)	n.d.	1.2
2	2.8	1.8
3	890	26
4	3.0	7.2
5	5.7	12
6	710	60
Staurosporine	1.0	10

b

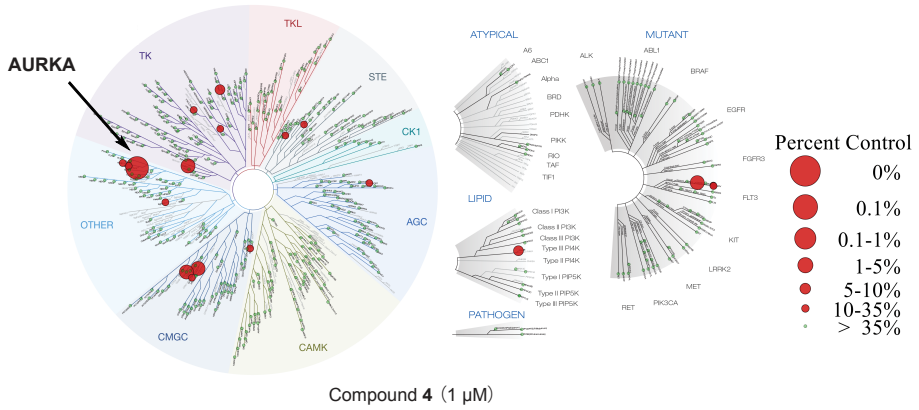

Compound **4** (1 μM)

c

4	%Ctrl @ 1μM	K_d (nM)	IC_{50} (nM)
Aurora A	0.1	6.3	3.0
Aurora B	13	160	22
Aurora C	32	43	13
CDK4-CyclinD1	3.3	52	7.2
CDK4-CyclinD3	1.5	17	12
CDK6-CyclinD1	n.d.	n.d.	27
CDK9	3.0	6.3	1.8
CDK13	11	210	n.d.
EPHB6	4.5	150	n.d.
PI4KB	5.3	220	n.d.
ROCK1	19	>3,000	n.d.
TNK1	13	610	n.d.
TRKA	5.3	24	86

d

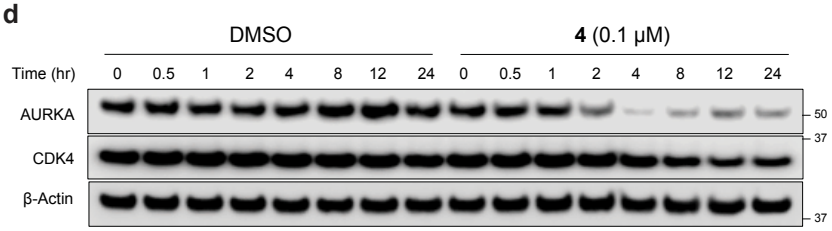

e

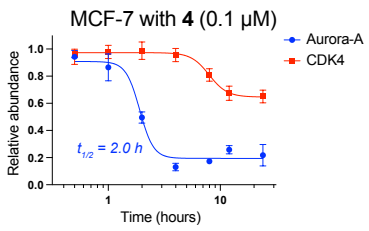

f

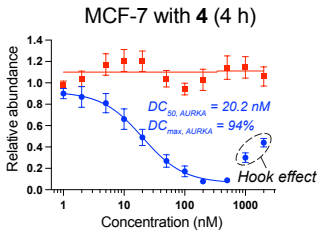

g

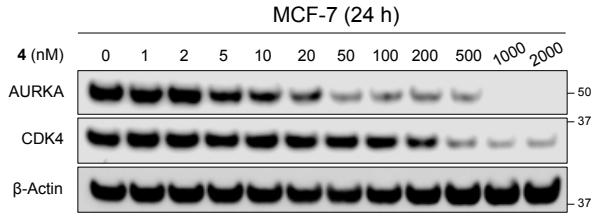

h

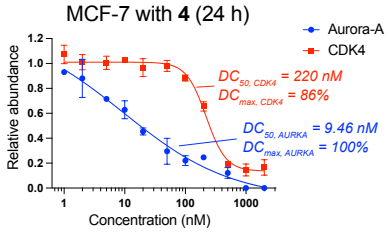

i

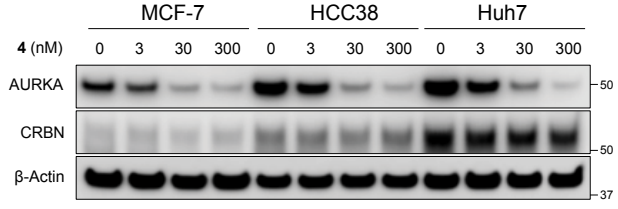

j

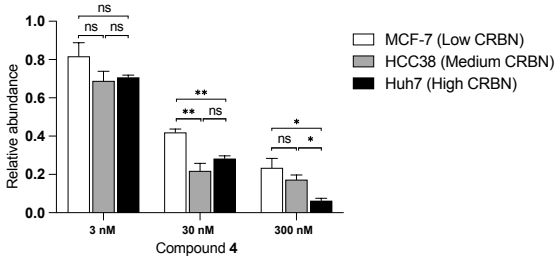

Extended data Figure 1 | Discovery of novel Aurora-A degraders. **a**, Kinase inhibitory activities (IC_{50}) against Aurora-A and CDK4-Cyclin D1. Staurosporine: a potent and broad-spectrum protein kinase inhibitor as a positive control. Data are the average of two independent biological replicates. **b.** Full spectrum of the KINOMEscan TREEspot map demonstrating the selectivity profiles of **4** against a panel of 468 kinases. See Supplementary Table 2 for a full list of kinases tested. **c**, The binding affinity (K_d) and kinase inhibitory activities (IC_{50}) of compound **4** for kinase targets with %Control <20% from the KINOMEscan. Data are the average of two independent biological replicates. **d-e**, **4** (0.1 μM) induces a potent and selective degradation of Aurora-A in a time-dependent manner in MCF-7 cells. Figure **d** is a representative figure of four biological replicates. **f**, Degradation curves of Aurora-A and CDK4 corresponding to **Fig. 1e**. **g-h**, **4** induced the degradation of Aurora-A and CDK4 in MCF-7 cells after 24 h. n = 2. **i-j**, Aurora-A degradation by **4** in three cell lines that have different CRBN expression levels. n = 3. Degradation curves/bars represent mean ± s.e.m from aggregated data. *p < 0.05, **p < 0.01.

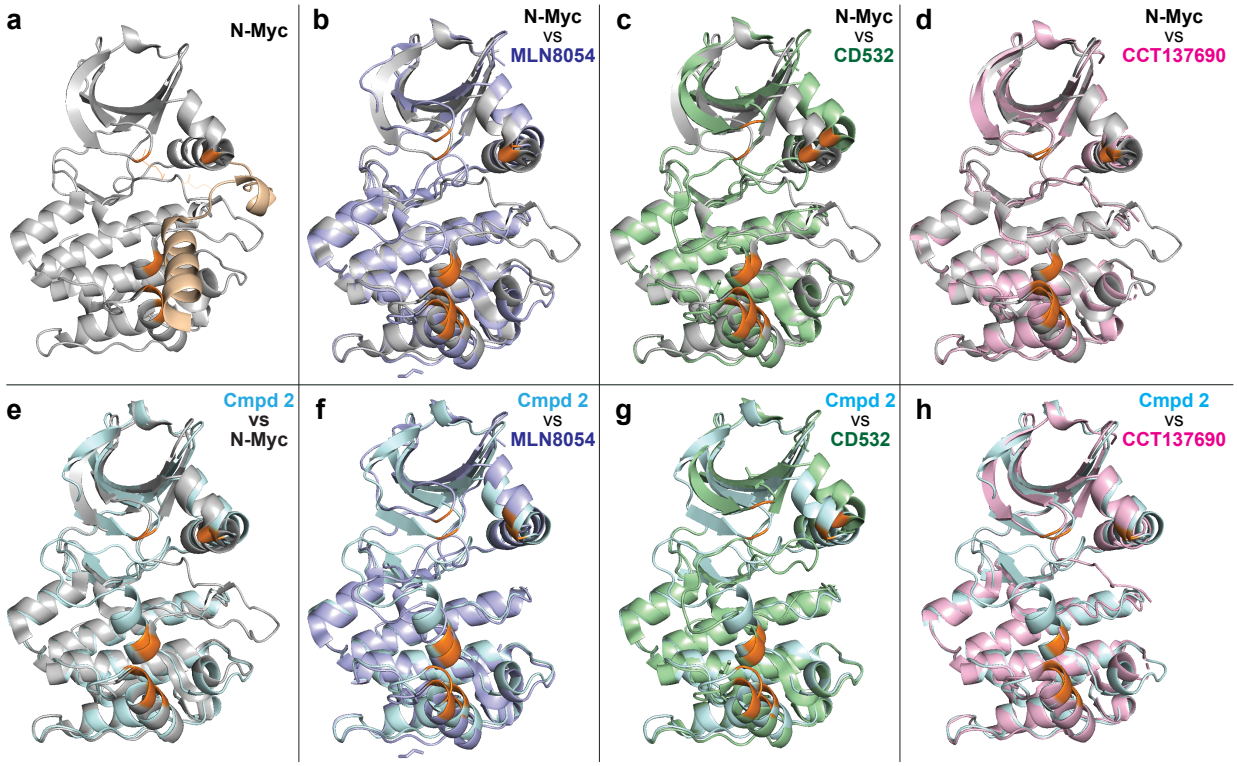

Extended data Figure 2 | Superposition of Aurora-A structures when co-crystallized with N-Myc or inhibitors. **a**, Aurora-A structure with N-Myc peptide (PDB: 5G1X, grey); **b**, Aurora-A/N-Myc vs Aurora-A/MLN8504 (PDB: 2WTV, blue); **c**, Aurora-A/N-Myc vs Aurora-A/CD532 (PDB: 4J8M, green); **d**, Aurora-A/N-Myc vs Aurora-A/CCT137690 (PDB: 2X6E, pink); **e**, Aurora-A/N-Myc vs Aurora-A/**2** (PDB: To Be Provided, cyan); **f**, Aurora-A/**2** vs Aurora-A/MLN8504; **g**, Aurora-A/**2** vs Aurora-A/CD532; **h**, Aurora-A/**2** vs Aurora-A/CCT137690. Key residues on Aurora-A that directly interacts with N-Myc peptide are highlighted in orange. CCT137690: a DFG-in Aurora-A inhibitor bound to the active state of Aurora-A.

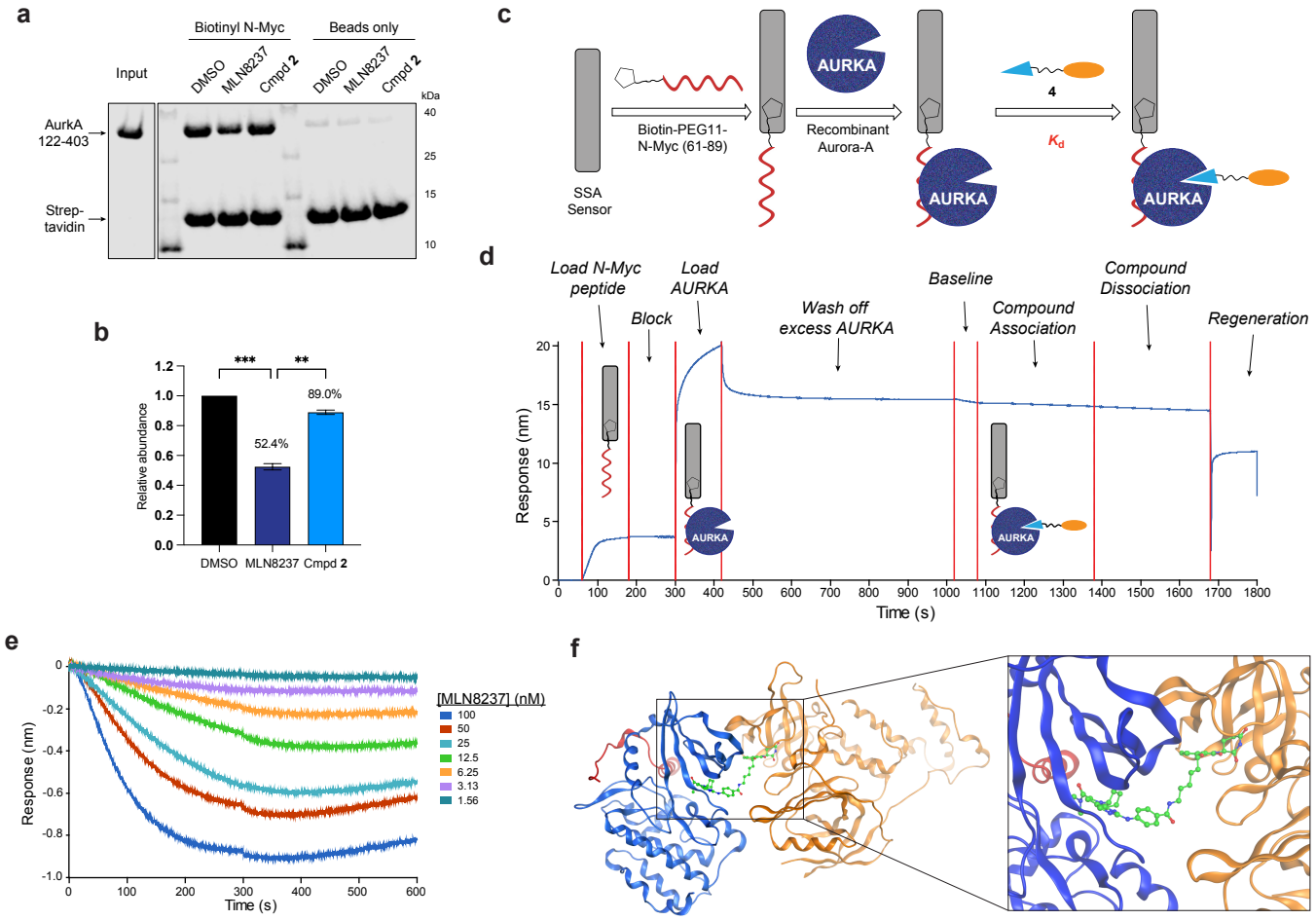

Extended data Figure 3 | Biophysical assays to demonstrate the target engagement of 2 and 4 binds with the Aurora-A/N-Myc. a-b. *In vitro* pull-down assay with recombinant Aurora-A and biotinylated N-Myc 61-89 peptide. n = 2. Bars represent mean ± s.d. **p < 0.01, ***p < 0.001. **c-d.** The set-up and workflow of the BLI ternary binding assay. **e**, BLI ternary binding assay with MLN8237 shows the disruption of the biotinylated N-Myc peptide/Aurora-A complex. n = 2. **f.** Computational modeling of the N-Myc/4/Aurora-A/CRBN complex. The peptide from N-Myc is shown in red, Aurora-A in blue, **4** in green, and CRBN in orange.

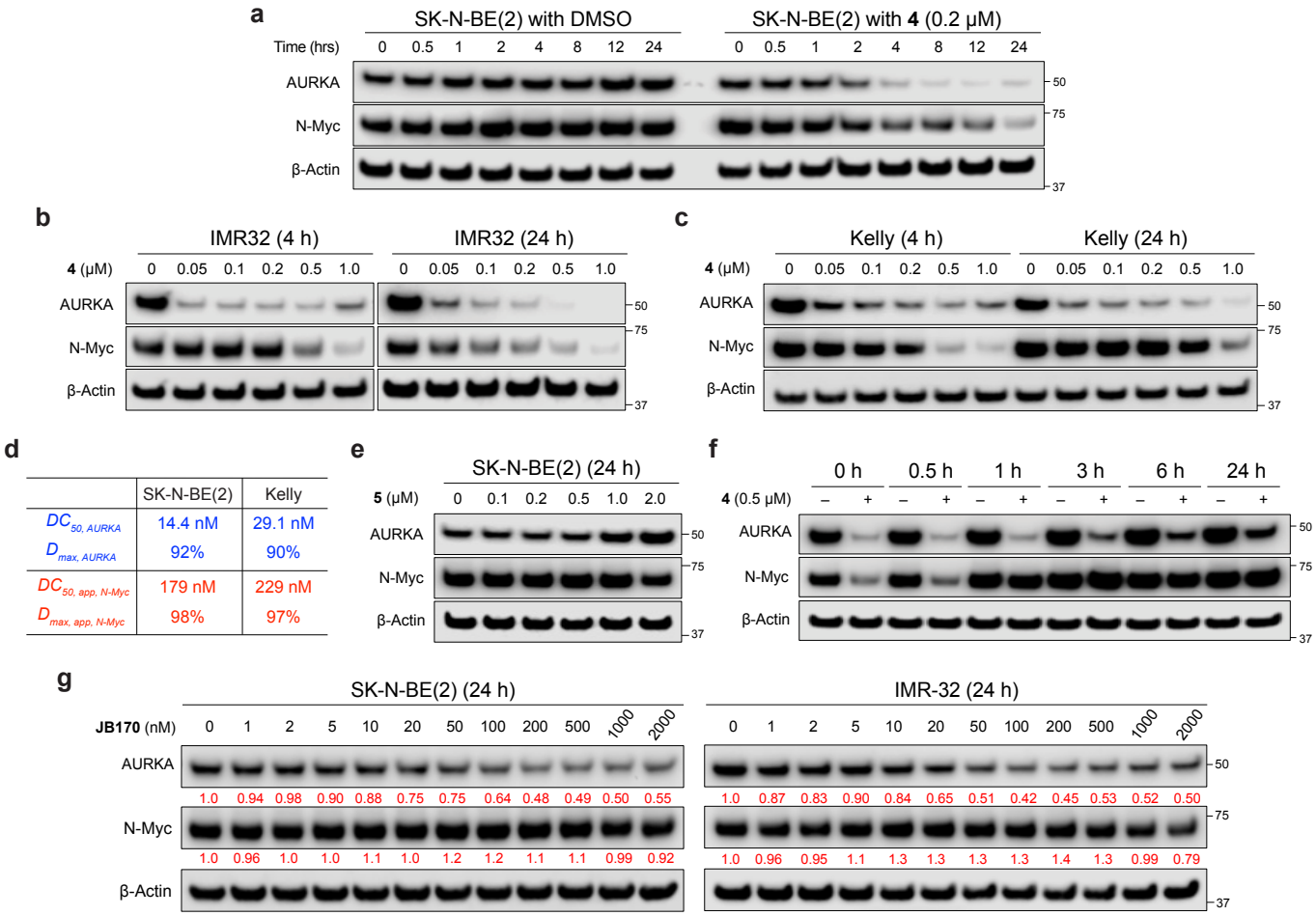

Extended data Figure 4 | 4 induces N-Myc degradation in *MYCN*-amplified NB cells. a, **4** (0.4 μM) time-dependently induces the degradation of Aurora-A and N-Myc in SK-N-BE(2) cells. n = 3. **b-c**, Concomitant degradation of Aurora-A and N-Myc by **4** in IMR-32 cells (**c**) and Kelly cells (**d**) after 4 h and 24 h. n = 3. **d**, DC_{50} and D_{max} values from Figures **2b** and **2c**, data are average of three biological replicates. **e**, Inactive PROTAC **5** did not affect the protein levels of Aurora-A and N-Myc in SK-N-BE(2) cells after 24 h. n = 4. **f**, Washout experiment in SK-N-BE(2). Cells were pre-treated with **4** for 4 h, and the moment when replaced with fresh media was marked as 0 h. Cell lysates were collected at the following indicated time points. n = 3. **g**, JB170 induced Aurora-A degradation with a low D_{max}, and did not degrade N-Myc in SK-N-BE(2) and IMR-32 cell lines after 24 h. n = 3.

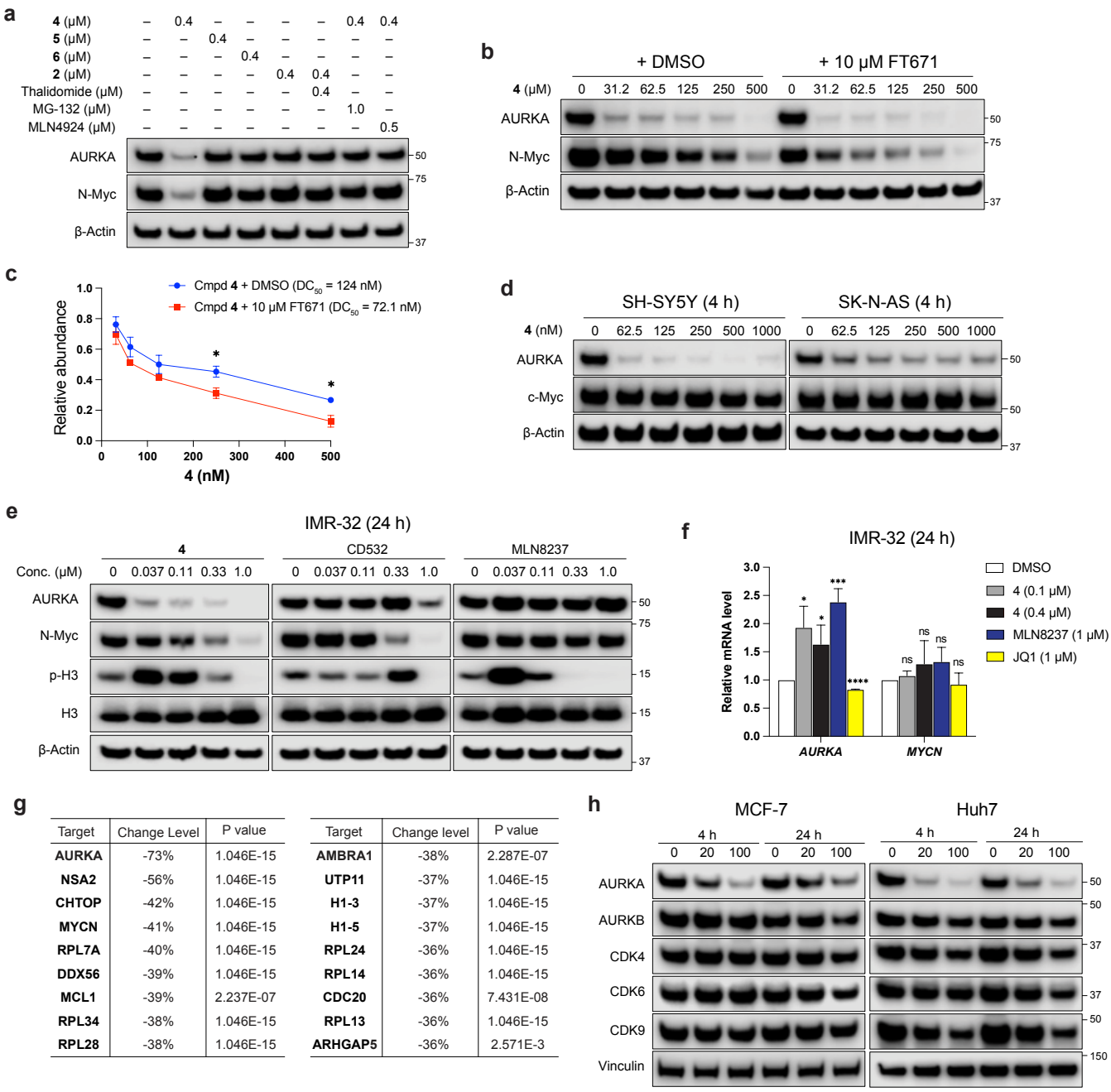

g

Target	Change Level	P value	Target	Change level	P value
AURKA	-73%	1.046E-15	**AMBRA1**	-38%	2.287E-07
NSA2	-56%	1.046E-15	**UTP11**	-37%	1.046E-15
CHTOP	-42%	1.046E-15	**H1-3**	-37%	1.046E-15
MYCN	-41%	1.046E-15	**H1-5**	-37%	1.046E-15
RPL7A	-40%	1.046E-15	**RPL24**	-36%	1.046E-15
DDX56	-39%	1.046E-15	**RPL14**	-36%	1.046E-15
MCL1	-39%	2.237E-07	**CDC20**	-36%	7.431E-08
RPL34	-38%	1.046E-15	**RPL13**	-36%	1.046E-15
RPL28	-38%	1.046E-15	**ARHGAP5**	-36%	2.571E-3

Extended data Figure 5 | 4 induces N-Myc degradation in *MYCN*-amplified NB cells. a, Mechanistic studies of N-Myc degradation by **4** after 4 h. For the two lanes on the right side, cells were pre-treated with MG-132 (1.0 μM) or MLN4924 (0.5 μM) for 1 h before adding **4** (0.1 μM) for another 4 h. n = 3. **b-c**, Synergistic effects on N-Myc degradation through co-treatment of **4** with FT671 (10 μM) for 24 h in IMR-32 cells. n = 3. Degradation curves (**c**) represent mean ± s.e.m. **d**, **4** induces degradation of Aurora-A but not c-Myc in *MYCN*-non-amplified NB SH-SY5Y and SK-N-AS cells after 4 h. n = 3. **e**, Head-to-head comparison of **4** with MLN8237 and CD532 for their effects on the protein level changes of Aurora-A, N-Myc, p-H3 in IMR-32 cells after 24 h. n = 3. **f**, Relative mRNA levels of *AURKA* and *MYCN* in IMR-32 cells after the treatment with **4**, MLN8237, or a BET inhibitor JQ1 for 24 h by RT-qPCR. n = 3. Bars represent mean ± s.d. *p < 0.05, ***p < 0.001, ****P < 0.0001. **g**, Protein targets that were decreased by > 35% from the TMT-based quantitative proteomic profiling of **4** in Figure **3f**. **h**, Immunoblotting of Aurora-A and other kinases in non-NB MCF-7 and Huh7 cells after the treatment with **4** for 4 h and 24 h. n = 3.

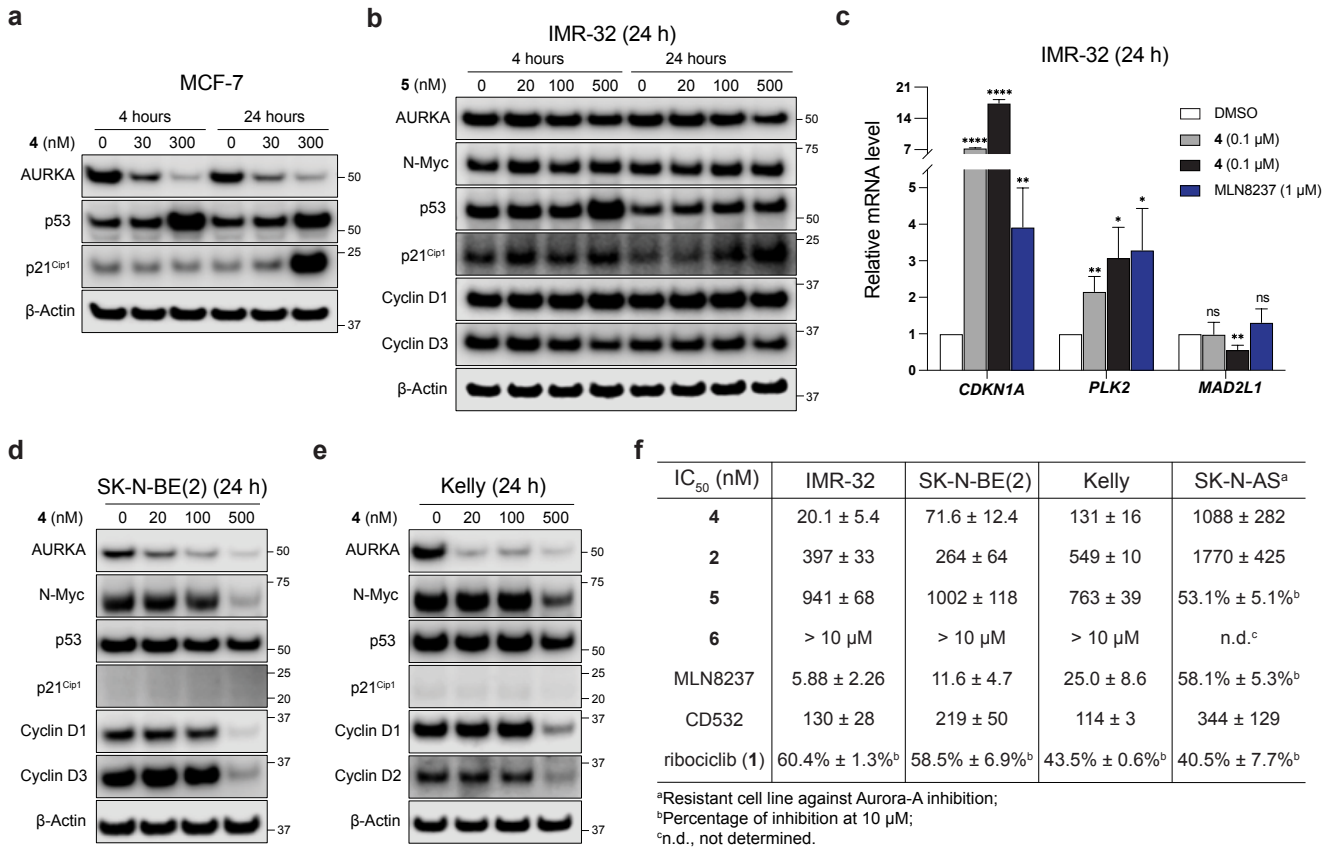

f

IC_{50} (nM)	IMR-32	SK-N-BE(2)	Kelly	SK-N-AS[a]
4	20.1 ± 5.4	71.6 ± 12.4	131 ± 16	1088 ± 282
2	397 ± 33	264 ± 64	549 ± 10	1770 ± 425
5	941 ± 68	1002 ± 118	763 ± 39	53.1% ± 5.1%[b]
6	> 10 μM	> 10 μM	> 10 μM	n.d.[c]
MLN8237	5.88 ± 2.26	11.6 ± 4.7	25.0 ± 8.6	58.1% ± 5.3%[b]
CD532	130 ± 28	219 ± 50	114 ± 3	344 ± 129
ribociclib (**1**)	60.4% ± 1.3%[b]	58.5% ± 6.9%[b]	43.5% ± 0.6%[b]	40.5% ± 7.7%[b]

[a]Resistant cell line against Aurora-A inhibition;
[b]Percentage of inhibition at 10 μM;
[c]n.d., not determined.

Extended Data Figure 6 | *In vitro* and *in vivo* therapeutic effects of 4 for NB. a. 4 upregulates tumor suppressor proteins p53 and $p21^{Cip1}$ in $TP53^{wt}$ MCF-7 cells after 24 h. n = 3. **b.** Immunoblotting of the signaling components in the p53 and N-Myc pathways after the treatment with the inactive PROTAC **5** in IMR-32 cells after 24 h. n = 3. **c**, Relative mRNA levels of *CDKN1A* and *PLK2* as p53 targeting genes, and *MAD2L1* as a N-Myc direct target gene in IMR-32 cells after 24 h. n = 3. *p < 0.05, **p < 0.01, ****P < 0.0001. **d-e**, Immunoblotting of the signaling components in the p53 and N-Myc pathways after the treatment with **4** in *TP53* mutant SK-N-BE(2) and Kelly cell lines after 24 h. n = 3. **f**. Cytotoxicity of compounds in *MYCN*-amplified and MYCN-non-amplified NB cells. n = 3. Data represent mean ± s.d.